Pairing correlations in the rotating nucleus discussed within the generator coordinate method

W. Satuła
Institute of Theoretical Physics, Warsaw University, ul. Hoża 69, PL-00-681 Warsaw, Poland and Manne Siegbahn Institute of Physics, Frescativägen 24, S-10405 Stockholm, Sweden

W. Nazarewicz
Institute of Physics, Warsaw University of Technology, ul. Koszykowa 75, PL-00-662 Warsaw, Poland and Institute of Theoretical Physics, Warsaw University, ul. Hoża 69, PL-00-681 Warsaw, Poland

Z. Szymański
Institute of Theoretical Physics, Warsaw University, ul. Hoża 69, PL-00-681 Warsaw, Poland and Institut des Sciences Nucléaires 53, avenue des Martyrs, F-38026 Grenoble CEDEX, France

R. Piepenbring
Institut des Sciences Nucléaires 53, avenue des Martyrs, F-38026 Grenoble CEDEX, France
(Received 2 August 1989)

The influence of nuclear rotation on pairing correlations is discussed using a simple solvable two-level model. Exact solutions are compared to approximate ones obtained with the generator coordinate method both with and without particle-number projection. The collective subspace associated with the generator coordinates used has a finite dimension and it can be exactly separated from the full Hilbert space of the generating functions. Analytical formulas for the norm matrix and Hamiltonian kernels are obtained. It is shown that the generator coordinate method improves considerably the calculations based on the random-phase-approximation approach, in particular near the critical frequency where the pairing gap collapses.

I. INTRODUCTION

Understanding the mechanism of the rapid changes occurring in the nuclear structure has always been one of the most fascinating challenges in nuclear physics. It often happens that a well established and relatively well investigated nuclear coupling scheme tends to change suddenly under some external conditions in favor of an entirely different picture. This is sometimes referred (correctly or incorrectly) to as phase transition. Although the initial and final states of such a transition are relatively well understood the theoretical treatment that follows closely the full transition process is, in general, difficult to carry on and thus remains rather obscure.

It is, therefore, important to search for such an approach that remains valid not only before and after the transition but is also able to carry on all the way through the whole process of the change in the coupling scheme. We intend to investigate to what extent the method of a generator coordinate is able to play such a role. In particular, the often discussed but—in our opinion—not yet fully understood process of the disappearance of the pairing superfluid correlations in a fast rotating nucleus may become a favorable test case. It has been established (see, e.g., Refs. 1 and 2) that at low rotational frequencies ω the short-range pairing force is strong enough to produce a coupling scheme which characterizes the existence of static-type superfluid correlations between the nucleons (also referred to sometimes as the Cooper-paris condensate). In the well known BCS approximation such a coupling scheme is represented as a nonvanishing value of the energy-gap parameter Δ. Furthermore, the lowest excited 0^+ states can be interpreted in many cases as some mixtures of shape and pairing vibrations in the superfluid system. They are successfully described by the random phase approximation (RPA).

On the other hand, at very high rotational frequencies ω the static-pairing coupling scheme seems to be destroyed ($\Delta \approx 0$) due to the Coriolis and centrifugal interactions.[3] Nevertheless, one may attempt to describe some of the low lying excitations of the system as dynamical pairing vibrations[4–6] possibly modified by the influence of the long-range component of the nucleon-nucleon force. Again, the RPA method may present itself as a good description of the resulting coupling scheme.

At some—perhaps narrow—region of the rotational frequency ω we expect the static pairing coupling scheme to disappear in favor of the rotating mean field with particle rather than quasiparticle elementary excitations. Unfortunately, it turns out that in the transition region the RPA formalism becomes entirely helpless in giving account of what is going on in the actual nuclear system (cf. for example Refs. 7 and 8). There have been some attempts made to overcome this difficulty and to understand the nuclear structure in this transition region. For example, in the calculations of Ref. 9 the transition region has been analyzed in terms of the boson-expansion technique. The approaches of this type brought rather satisfactory results in the framework of a simplified nuclear model. Nevertheless, they may become rather difficult when going over to a more realistic description

of the nucleus. Recently, an extensive analysis[10] of the possible disappearance of pairing correlations has been performed in terms of the fluctuations in the pairing field induced by a fast rotation. An updated list of relevant works on this subject can be found therein and in Ref. 11.

The pathologies of the mean field approach around the pairing collapse region can be cured by means of projection techniques. The particle-number projection method before variation (PNP) has been used for many years for description of pairing correlations at high spins (see, e.g., Refs. 10–12 and references quoted therein).

Another possible way for treating the pairing problem is offered by the generator coordinate method (GCM). In this case the most important fluctuations are treated fully quantum mechanically without restriction to small amplitudes, like the RPA method. In the absence of rotation the GCM was proven to give a good description of the lowest pairing excitations.[13–23]

The aim of this paper is to investigate the GCM as a candidate for a formalism that is able to replace the RPA and carry on the adequate description all the way through the transition region. We intend to lead our analysis in the framework of a solvable two-level nuclear model[24–26] where both the mean field [Hartree-Fock-Bogolyubov (HFB) plus RPA] and the exact solutions can be easily found and employed. Having at our disposal the simple model with easily ac-cessible exact solutions we thus hope to be able to estimate to what degree is the GCM capable to provide the adequate description of the process involving rapid changes in nuclear structure.

Within the model considered in this article the GCM can be performed explicitly which is rather unique case. The collective subspace has a finite dimension and the integral kernels have very simple analytical forms. Because all the steps of the GCM can be clearly show in the simple model, we think that it contains a big dose of didactics. For this reason we discuss it in a rather detailed way.

In Sec. II the GCM formalism is shortly reviewed. Section III presents the different variants of the model and the related numerical results are given in Sec. IV. Finally, the conclusions are contained in Sec. V.

II. THE GENERATOR COORDINATE METHOD

In this section a short sketch of the GCM is given. Our presentation and notation follows mostly that of Ref. 12.

The GCM trial wave function Ψ is based on the superposition of the wave functions $\Phi(\bar{a})$ (generating functions) depending parametrically on a set of continuous parameters (generator coordinates) $\bar{a}$:

$$\Psi=\int d\bar{a}\, f(\bar{a})\Phi(\bar{a}) . \tag{1}$$

The weight function $f(\bar{a})$ can be determined from the Ritz variational principle, which leads to the integral equation,

$$\int d\bar{a}\, f(\bar{a})H(\bar{a},\bar{a}')=E\int d\bar{a}\, f(\bar{a})N(\bar{a},\bar{a}') , \tag{2}$$

known as the Griffin-Hill-Wheeler equation (GHW).[27,28] Here $H(\bar{a},\bar{a}')$ and $N(\bar{a},\bar{a}')$ denote the integral kernels of the Hamiltonian and the norm matrix, respectively. The linear dependence of the generating functions requires the orthogonalization of the $\Phi(\bar{a})$ set which can be performed using the so-called symmetric orthogonalization method. In this method one has to solve the eigenvalue problem for the norm matrix

$$\int d\bar{a}'N(\bar{a},\bar{a}')u_k(\bar{a}')=n_k u_k(\bar{a}) , \tag{3}$$

where the eigenfuntions $u_k(\bar{a})$ form a complete orthogonal set of functions in the space of the weight functions $f(\bar{a})$. By means of the eigenfunctions $u_k(\bar{a})$ having nonzero eigenvalues ($n_k>0$) one can construct the so-called "natural states",

$$|k\rangle=\frac{1}{\sqrt{n_k}}\int d\bar{a}u_k(\bar{a})\Phi(\bar{a}) , \tag{4}$$

spanning the collective subspace. The diagonalization of the Hamiltonian projected onto the collective subspace leads to the eigenvalue problem

$$\sum_{k'}\langle k|H|k'\rangle g_{k'}=E_k g_k , \tag{5}$$

with

$$\langle k|H|k'\rangle=\frac{1}{\sqrt{n_k n_{k'}}}\int d\bar{a}\int d\bar{a}'u_k^*(\bar{a})H(\bar{a},\bar{a}')u_{k'}(\bar{a}') . \tag{6}$$

The weight functions are finally given by

$$f(\bar{a})=\sum_k\frac{g_k}{\sqrt{n_k}}u_k(\bar{a}) . \tag{7}$$

The formalism presented above can be solved analytically only for the simplest physical models. Therefore, numerical methods have been developed[12,21] to solve the GHW equation. We apply here the method of the discretization of the integrals. It resolves itself into the formal replacement of the integrals by the sums over whole set of mesh points, changing the integral equations into the matrix equations. The diagonalization of the norm matrix (3) allows us to construct the collective subspace spanned by eigenfunctions $u_k(\bar{a})$ having eigenvalues n_k greater than given small positive number. This procedure has to be repeated, taking more and more mesh points for discretization, to obtain the convergence in the eigenvalues E_k (see also a recent paper[29]).

III. APPLICATION TO THE SOLVABLE NUCLEAR MODELS

A. Description of the model

In this section we intend to apply the GCM to the solution of a simple two-level model. Our model consists of a $j=\frac{3}{2}$ multiplet embedded in a prolate-deformed mean field which produces a splitting of the multiplet into two levels with $m=\pm\frac{3}{2}$ (upper level, energy $+\epsilon$) and $m=\pm\frac{1}{2}$ (lower level, energy $-\epsilon$). The whole multiplet is repeated

Ω times. The number of particles filling these level is assumed to be equal 2Ω thus corresponding to the one-half of all the available 4Ω states. As the residual interaction we introduce a short-range monopole pairing force of a strength G and a long-range quadrupole-quadrupole interaction of a strength χ that corresponds to the Y_{20} multipole component i.e., the one associated with the axially symmetric β vibrations. In the present study two versions of the model have been employed. In the simpler version (Sec. III B) rotation is neglected. In the second version (Sec. III C) the familiar cranking term $-\omega j_x$ has also been added. This term corresponds to the rotation of the whole system with the constant angular velocity ω about a fixed axis in space (here: x axis). Finally, in Sec. III D the particle-number symmetry conserving formalism is presented. The model employed in the present paper becomes thus the SO(5) version of the model described in Refs. 24 and 30 as applied to the cranking model instead of that of a particle plus rotor. The same version of the model has been used in Refs. 6 and 26 although in the present case the Q-Q forces have also been allowed [cf. Ref. 31 where also the Q-Q force has been used, however, without rotation thus leading to the SO(4) symmetry].

The model can be solved exactly by means of the group theory and we shall take advantage of this by comparing the exact solutions with those derived in the various version obtained within the framework of GCM.

B. A simple version of the model ($\omega=0$)

Let us begin our discussion with the case of a nonrotating system. This seems to form a good pedagogical introduction to the more complex case discussed subsequently in Sec. III C. In this case the only interesting feature of the model is related to the competition between the pairing force and the mean field as represented by a tendency to locate the particles in the lowest possible energy levels.

First of all let us define the relevant ingredients of the two-level model in this version. The matrix elements of the pairing force are given by

$$\bar{v}^{(P-P)}_{lmpq} = -G\,\mathrm{sgn}(l)\,\mathrm{sgn}(p)\delta_{l\bar{m}}\delta_{p\bar{q}}\ , \tag{8}$$

where $\bar{m}$ denotes time reversed state m [$\mathrm{sgn}(\bar{m})=-\mathrm{sgn}(m)$]. The antisymmetrized matrix element of the Q-Q force writes

$$\bar{v}^{(Q-Q)}_{lmpq} = -\chi(q_{lp}q_{mq}-q_{lq}q_{mp})\ , \tag{9}$$

with

$$q_{11}=q_{22}=-q_{33}=-q_{44}=-q\ . \tag{10}$$

The above two-body matrix elements have now to be completed by the one-body field. The single-particle matrix elements of the two-level model are

$$\epsilon_1=\epsilon_2=-\epsilon_3=-\epsilon_4=\epsilon\ . \tag{11}$$

In this variant, the two-level model is reduced to the Lipkin model discussed in detail in Sec. 10.3 of Ref. 12. In the case of the particle-hole-like interaction the Lipkin model can be solved exactly using the GCM with the trial wave function parametrized by only one generator coordinate[12] φ. In the case of pairing interaction one could try to introduce the pairing gap as a generator coordinate. However, it is more convenient to introduce another parameter, an angle φ, for this purpose. Indeed, for the half-filled shells, the (u,v) coefficients of the BCS wave function,

$$|\Phi\rangle=\prod_i (u_i+v_i c_i^{\dagger}c_{\bar{i}}^{\dagger})|0\rangle\ , \tag{12}$$

obey the relations

$$u_{\mathrm{up}}=v_{\mathrm{low}}=\frac{1}{\sqrt{2}}\left[1+\frac{\epsilon}{E}\right]^{1/2},\qquad v_{\mathrm{up}}=u_{\mathrm{low}}=\frac{1}{\sqrt{2}}\left[1-\frac{\epsilon}{E}\right]^{1/2}, \tag{13}$$

where $E=(\epsilon^2+\Delta^2)^{1/2}$.

Thus, guided by the above relations it seems reasonable to introduce the angle φ as

$$v_{\mathrm{low}}=u_{\mathrm{up}}=\cos\frac{\varphi}{2},\quad u_{\mathrm{low}}=v_{\mathrm{up}}=\sin\frac{\varphi}{2}\ , \tag{14}$$

instead of Eq. (13). In the BCS approximation the angle φ has a well defined value given by

$$\tan\varphi=\frac{\Delta}{\epsilon},\quad \text{or}\quad \sin\varphi=\frac{\Delta}{G\Omega}\ . \tag{15}$$

In the next step one can calculate the integral kernels $N(\varphi,\varphi')$ and $H(\varphi,\varphi')$. It turns out that in the case of the two-level model the calculations can be performed explicitly and they lead to simple closed form expressions analogous to those from[12]

$$N(\varphi,\varphi')=\left[\cos\left[\frac{\varphi-\varphi'}{2}\right]\right]^{2\Omega} \tag{16}$$

$$\frac{H(\varphi,\varphi')}{N(\varphi,\varphi')}=-2\epsilon\Omega\left[\frac{\cos[(\varphi+\varphi')/2]}{\cos[(\varphi-\varphi')/2]}\right]-\frac{1}{2}G\Omega\left\{2\Omega\left[\frac{\sin[(\varphi+\varphi')/2]}{\cos[(\varphi-\varphi')/2]}\right]^2+\frac{\cos\varphi\cos\varphi'}{\{\cos[(\varphi-\varphi')/2]\}^2}+\frac{1}{\{\cos[(\varphi-\varphi')/2]\}^2}\right\}$$
$$-\chi q^2\Omega(2\Omega-1)\left[\frac{\cos[(\varphi+\varphi')/2]}{\cos[(\varphi-\varphi')/2]}\right]^2\ . \tag{17}$$

The eigenfunctions of the overlap matrix (16) can be easily found as plane waves:

$$\Phi_k = \frac{1}{\sqrt{2\pi}} \exp(ik\varphi) , \tag{18}$$

with the eigenvalues

$$n_k = \frac{2\pi}{2^{2\Omega}} \begin{bmatrix} 2\Omega \\ \Omega + k \end{bmatrix} , \tag{19}$$

where $k = -\Omega, -\Omega+1, \ldots, \Omega$. The collective subspace has, therefore, a finite dimension of $2\Omega+1$. Consequently, the matrix elements of the Hamiltonian (6) can be found in a closed form,

$$\begin{aligned} H_{k,k'} = & -\epsilon(f_k \delta_{k,k'-1} + f_{-k}\delta_{k,k'+1}) \\ & - \frac{G}{4(2\Omega-1)} \{[4\Omega(\Omega^2-k^2)+2(3\Omega^2-\Omega-k^2)]\delta_{k,k'} - (2\Omega-1)(f_k f_{k+1}\delta_{k,k'-2} + f_{-k}f_{-k+1}\delta_{k,k'+2})\} \\ & - \tfrac{1}{2}\chi q^2 \{2(\Omega^2-k^2)\delta_{k,k'} + (f_k f_{k+1}\delta_{k,k'-2} + f_{-k}f_{-k+1}\delta_{k,k'+2})\} , \end{aligned} \tag{20}$$

where

$$f_k = [(\Omega+k+1)(\Omega-k)]^{1/2} . \tag{21}$$

Diagonalizing the energy matrix (20) we obtain the $2\Omega+1$ eigenenergies of our problem in the GCM approximation. They should, in principle, be compared with the eigenvalues of the exact solution. However, in the exact solution of the two-level model we would like to identify the collective subspace as corresponding to the states characterized by the $(\Omega+1)$ dimensional symmetric representation of the corresponding SO(4) group (see, e.g., Ref. 31). In order to solve this discrepancy let us observe that the GCM apart from the usual symmetry (following from the hermiticity of the Hamiltonian),

$$H(\varphi,\varphi') = H(\varphi',\varphi) , \tag{22}$$

obeys an additional symmetry. This symmetry is reflected by the following feature of the Hamiltonian kernels:

$$H(\varphi,\varphi') = H(-\varphi,-\varphi') . \tag{23}$$

Thus instead of eigenstates (18) one can employ their symmetric and antisymmetric combinations,

$$\Psi_k^{(s)} = \frac{1}{\sqrt{2(1+\delta_{k,0})}} (\Phi_k + \Phi_{-k}) , \tag{24}$$

$$\Psi_k^{(a)} = \frac{1}{\sqrt{2}} (\Phi_k - \Phi_{-k}) . \tag{25}$$

It follows from the additional symmetry (23) that the matrix $H_{k,k'}$ becomes block diagonal when transformed to the new representation, i.e., the $(2\Omega+1)$ representation space of the GCM breaks down into two distinct subspaces of the symmetric and antisymmetric states, respectively, according to the schematic decomposition

$$(2\Omega+1) = (\Omega+1) \oplus (\Omega) . \tag{26}$$

It seems natural to keep only the symmetric part of this space as its dimensions corresponds to that of the exact solution of the model. Indeed, a closer examination of the antisymmetric states of Eq. (25) exhibits their unphysical picture: They do not contain the wave function component characterized by the correct number of particles ($N = 2\Omega$).

C. The full version of the model ($\omega \neq 0$)

Let us now discuss the more general version of the two-level model including, in addition to the previous variant discussed above, the cranking term $-\omega j_x$. The corresponding Hamiltonian in the rotating frame (Routhian) reads

$$H^{\omega} = H_{\text{s.p.}} + H_{\text{pair}} + H_{QQ} - \omega j_x . \tag{27}$$

In this case, the GCM becomes more complicated. We shall employ the formalism of a transformation from the one given HFB picture of quasiparticles characterized by the creation and annihilation operators $(\alpha^\dagger, \alpha)$ to another HFB picture characterized by the operators $(\alpha'^\dagger, \alpha')$. This transformation is known as the Onishi formula (Refs. 12 and 32). The quasiparticle representations $(\alpha^\dagger, \alpha)$ and $(\alpha'^\dagger, \alpha')$ correspond to the two different Bogolyubov transformations,

$$\begin{bmatrix} \alpha^\dagger \\ \alpha \end{bmatrix} = \begin{bmatrix} A^T & B^T \\ B^\dagger & A^\dagger \end{bmatrix} \begin{bmatrix} c^\dagger \\ c \end{bmatrix} , \tag{28}$$

and

$$\begin{bmatrix} \alpha'^\dagger \\ \alpha' \end{bmatrix} = \begin{bmatrix} A'^T & B'^T \\ B'^\dagger & A'^\dagger \end{bmatrix} \begin{bmatrix} c^\dagger \\ c \end{bmatrix} , \tag{29}$$

derive from the same picture of particle operators $(c^\dagger, c)$. Thus the transformation from one picture given by (28) to another (29) can be accomplished by

$$\begin{bmatrix} \alpha^\dagger \\ \alpha \end{bmatrix} = \begin{bmatrix} U & V \\ V & U \end{bmatrix} \begin{bmatrix} \alpha'^\dagger \\ \alpha' \end{bmatrix} , \tag{30}$$

where the transformation matrix

$$\begin{bmatrix} U & V \\ V & U \end{bmatrix}$$

can be obtained from the original Bogolyubov matrices as

$$U = A^\dagger A' + B^\dagger B' , \tag{31}$$

$$V=B^T A'+A^T B \ .$$

Having found the matrices U and V the straightforward formulas for the overlap matrix and the integral kernels of the Hamiltonian can be given:

$$\langle \Phi'|\Phi\rangle=(\det U)^{1/2}=[\det(A^\dagger A'+B^\dagger B')]^{1/2} \ , \quad (32)$$

$$\frac{\langle \Phi'|H^\omega|\Phi\rangle}{\langle \Phi'|\Phi\rangle}=\mathrm{Tr}(e\rho^{(10)})+\tfrac{1}{2}\,\mathrm{Tr}_1\,\mathrm{Tr}_1(\rho^{(10)}\bar{v}\rho^{(10)}) +\tfrac{1}{4}\,\mathrm{Tr}_2\,\mathrm{Tr}_2(\kappa^{(01)*}\bar{v}\kappa^{(10)}) \ , \quad (33)$$

where the three matrices $\rho^{(10)}$, $\kappa^{(01)}$, and $\kappa^{(10)}$ are defined as[12]

$$\begin{aligned}\rho^{(10)}&=B^*(U^T)^{-1}B'^T \ ,\\ \kappa^{(01)*}&=-A(U^T)^{-1}B'^T \ ,\\ \kappa^{(10)}&=B^*(U^T)^{-1}A'^T \ .\end{aligned} \quad (34)$$

The meaning of the three terms occuring in (33) is usual:

$$\mathrm{Tr}(e\rho^{(10)})=\sum_{pq} e_{pq}\rho^{(10)}_{qp} \ , \quad (35)$$

$$\mathrm{Tr}_1\,\mathrm{Tr}_1(\rho^{(10)}\bar{v}\rho^{(10)})=\sum_{pqlm}\rho^{(10)}_{ml}\bar{v}_{lqmp}\rho^{(10)}_{pq} \ , \quad (36)$$

$$\mathrm{Tr}_2\,\mathrm{Tr}_2(\kappa^{(01)*}\bar{v}\kappa^{(10)})=\sum_{lmpq}\kappa^{(01)*}_{lm}\bar{v}_{lmpq}\kappa^{(10)}_{pq} \ . \quad (37)$$

Here e denotes the one-body part of H^ω (i.e., the $H_{\mathrm{s.p.}}$ as well as the cranking term) while $\bar{v}$ denotes the residual two-body interaction (the sum of pairing and quadrupole forces).

Now, we have to specify the generator coordinates relevant to a rotating system. The Bogolyubov transformation matrices corresponding to the Hartree-Fock-Bogolyubov-cranking (HFBC) [or rather RBCS (rotating BCS)] states have been given explicitly for the two-level model in Ref. 6. It is seen that for the rotating system one generator coordinate φ [corresponding roughly to the pairing gap Δ, cf. Eq. (15)] is not sufficient since one also has to deal with a nuclear rotation (characterized by the angular velocity ω). Thus we introduce now the two generator coordinates, angles φ and ψ that define the Bogolyubov matrices A and B. Using the abbreviated notation

$$c=\cos\frac{\varphi}{2}, \quad \bar{c}=\cos\frac{\psi}{2}, \quad s=\sin\frac{\varphi}{2}, \quad \bar{s}=\sin\frac{\psi}{2} \ , \quad (38)$$

we introduce the following parametrization of the matrices A and B:

$$A_{\nu j}=\frac{1}{\sqrt{2}}\begin{pmatrix} c & -c & 0 & 0\\ 0 & 0 & c & -\bar{c}\\ -s & -\bar{s} & 0 & 0\\ 0 & 0 & s & \bar{s}\end{pmatrix} ,$$

$$B_{\nu j}=\frac{1}{\sqrt{2}}\begin{pmatrix} 0 & 0 & s & -\bar{s}\\ -s & \bar{s} & 0 & 0\\ 0 & 0 & c & \bar{c}\\ c & \bar{c} & 0 & 0\end{pmatrix} . \quad (39)$$

Here, the first index ν in both the matrices A and B runs over the four values $\nu=1,2,3,4$ ($2=\bar{1}, 4=\bar{3}$) characterizing the original states of the two-level model while the second index j runs over the four solutions of the RBCS equations, i.e., $j=1,2,\bar{1},\bar{2}$ in the notation of Ref. 6.

For the other Bogolyubov transformation the matrices A' and B' are built in the same way from the angles φ' and ψ' instead of φ and ψ. In the particular case of RBCS and $\chi=0$ the new parameters φ and ψ can be related to the dynamical parameters of the two-level model by[6]

$$\begin{aligned}\cos\frac{\varphi}{2}&=\frac{1}{\sqrt{2}}\left[1+\frac{\epsilon}{E_+}\right]^{1/2} ,\\ \sin\frac{\varphi}{2}&=\frac{1}{\sqrt{2}}\frac{\Delta+\omega}{[E_+(E_++\epsilon)]^{1/2}} ,\\ \cos\frac{\psi}{2}&=\frac{1}{\sqrt{2}}\left[1+\frac{\epsilon}{E_-}\right]^{1/2} ,\\ \sin\frac{\psi}{2}&=\frac{1}{\sqrt{2}}\frac{\Delta-\omega}{[E_-(E_-+\epsilon)]^{1/2}} ,\end{aligned} \quad (40)$$

with

$$E_\pm=[\epsilon^2+(\Delta\pm\omega)^2]^{1/2} \ .$$

In the RBCS approximation the angles φ and ψ have well defined values given by the pairing gap and the angular momentum equations:

$$\tan\varphi+\tan\psi=\frac{2\Delta}{\epsilon}, \quad \tan\varphi-\tan\psi=\frac{2\omega}{\epsilon} \ . \quad (41)$$

Note that for $\varphi=\psi$ Eq. (41) reduces itself to Eq. (15). Now, in order to take into account the rotation one has to add the cranking term (cf. Refs. 24 and 30) $-\omega j_x$ where the operator j_x couples only the states $\nu=1$ to $\nu=3$ and $\nu=2$ to $\nu=4$ (observe that in this way we neglect the signature splitting term which would couple $\nu=3$ to $\nu=4$). The matrix representation of j_x thus becomes

$$(j_x)_{\nu\nu'}=\frac{1}{2}\begin{pmatrix} 0 & 0 & 1 & 0\\ 0 & 0 & 0 & -1\\ 1 & 0 & 0 & 0\\ 0 & -1 & 0 & 0\end{pmatrix} . \quad (42)$$

Relations (11) and (42) define the single-particle matrix element e entering Eq. (35). More explicitly,

$$e_{pq}=\epsilon_p\delta_{pq}-\omega(j_x)_{pq} \ . \quad (43)$$

With all these data we are now ready to calculate both the overlap matrix $N(\varphi',\psi';\varphi,\psi)$ and the energy matrix $H(\varphi',\psi';\varphi,\psi)$. Below, only the final results are given:

$$N(\varphi',\psi';\varphi,\psi)=\left[\cos\left[\frac{\varphi-\varphi'}{2}\right]\cos\left[\frac{\psi-\psi'}{2}\right]\right]^{\Omega}, \tag{44}$$

$$\begin{aligned}\frac{H(\varphi',\psi';\varphi,\psi)}{N(\varphi',\psi';\varphi,\psi)}=&-\epsilon\Omega\left[\frac{\cos[(\varphi+\varphi')/2]}{\cos[(\varphi-\varphi')/2]}+\frac{\cos[(\psi+\psi')/2]}{\cos[(\psi-\psi')/2]}\right]-\omega\Omega\left[\frac{\sin[(\varphi+\varphi')/2]}{\cos[(\varphi-\varphi')/2]}-\frac{\sin[(\psi+\psi')/2]}{\cos[(\psi-\psi')/2]}\right]\\&-\frac{1}{4}G\Omega\left[\Omega\left[\frac{\sin[(\varphi+\varphi')/2]}{\cos[(\varphi-\varphi')/2]}+\frac{\sin[(\psi+\psi')/2]}{\cos[(\psi-\psi')/2]}\right]^2\right.\\&\left.+\left\{\frac{\cos\varphi\cos\varphi'}{\cos^2[(\varphi-\varphi')/2]}+\frac{\cos\psi\cos\psi'}{\cos^2[(\psi-\psi')/2]}+2\frac{\cos[(\varphi-\psi)/2]\cos[(\varphi'-\psi')/2]}{\cos[(\varphi-\varphi')/2]\cos[(\psi-\psi')/2]}\right\}\right]\\&-\frac{1}{2}\chi q^2\Omega\left[\Omega\left[\frac{\cos[(\varphi+\varphi')/2]}{\cos[(\varphi-\varphi')/2]}+\frac{\cos[(\psi+\psi')/2]}{\cos[(\psi-\psi')/2]}\right]^2\right.\\&+\frac{1}{4}\left\{\frac{\sin\varphi\sin\varphi'}{\cos^2[(\varphi-\varphi')/2]}+\frac{\sin\psi\sin\psi'}{\cos^2[(\psi-\psi')/2]}-2\frac{\sin[(\varphi-\psi)/2]\sin[(\varphi'-\psi')/2]}{\cos[(\varphi-\varphi')/2]\cos[(\psi-\psi')/2]}\right\}\\&-\frac{3}{4}\left\{\left[\frac{\cos[(\varphi+\varphi')/2]}{\cos[(\varphi-\varphi')/2]}\right]^2+\left[\frac{\cos[(\psi+\psi')/2]}{\cos[(\psi-\psi')/2]}\right]^2\right\}\\&\left.-\frac{1}{2}\frac{\cos[(\varphi-\psi')/2]\cos[(\psi-\varphi')/2]}{\cos[(\varphi-\varphi')/2]\cos[(\psi-\psi')/2]}\right].\end{aligned} \tag{45}$$

Now, similarly as in the case of nonrotating system one may observe that the overlap matrix can be diagonalized analytically. The eigenfunctions become now the double plane waves with respect to the both parameters φ and ψ:

$$\Phi_{kl}(\varphi,\psi)=\frac{1}{2\pi}\exp[i(k\varphi+l\psi)], \tag{46}$$

with

$$-\frac{\Omega}{2}\le k\le\frac{\Omega}{2},\quad -\frac{\Omega}{2}\le l\le\frac{\Omega}{2}, \tag{47}$$

and the corresponding eigenvalues of the overlap matrix are

$$n_{kl}=\frac{(2\pi)^2}{2^{2\Omega}}\begin{pmatrix}\Omega\\(\Omega/2)+k\end{pmatrix}\begin{pmatrix}\Omega\\(\Omega/2)+l\end{pmatrix}. \tag{48}$$

One can now calculate the matrix elements $H_{k'l',kl}$ of $H(\varphi',\psi';\varphi,\psi)$ in the basis (46):

$$\begin{aligned}H_{k'l',kl}=&-(\epsilon+i\omega)(g_k\delta_{k,k'-1}\delta_{l,l'}+g_{l-1}\delta_{l,l'+1}\delta_{k,k'})\\&-(\epsilon-i\omega)(g_{k-1}\delta_{k,k'+1}\delta_{l,l'}+g_l\delta_{l,l'-1}\delta_{k,k'})\\&+\tfrac{1}{4}(G-2\chi q^2)[g_{k+1}g_k\delta_{k,k'-2}\delta_{l,l'}+g_{l+1}g_l\delta_{l,l'-2}\delta_{k,k'}+g_{k-1}g_{k-2}\delta_{k,k'+2}\delta_{l,l'}+g_{l-1}g_{l-2}\delta_{l,l'+2}\delta_{k,k'}\\&\qquad+2(g_kg_l\delta_{k,k'-1}\delta_{l,l'-1}+g_{k-1}g_{l-1}\delta_{k,k'+1}\delta_{l,l'+1})]\\&-\left[\frac{G(\Omega+1)+2\chi q^2\Omega}{2\Omega}\right](g_kg_{l-1}\delta_{k,k'-1}\delta_{l,l'+1}+g_{k-1}g_l\delta_{k,k'+1}\delta_{l,l'-1})\\&+\frac{1}{4}\left[(G+2\chi q^2)(2k^2+2l^2-\Omega^2)+G\left[\frac{4kl}{\Omega}-3\Omega\right]\right]\delta_{k,k'}\delta_{l,l'},\end{aligned} \tag{49}$$

where

$$g_k=\left[\begin{pmatrix}\Omega\\\frac{\Omega}{2}+k+1\end{pmatrix}\begin{pmatrix}\Omega\\\frac{\Omega}{2}-k\end{pmatrix}\right]^{1/2}. \tag{50}$$

The dimension of the collective subspace is now $(\Omega+1)^2$; see Eq. (47). This again exceeds the dimension of the corresponding space of the exact version of the two-level model which is now governed by the Lie algebra of the group SO(5) with the dimension $\frac{1}{2}(\Omega+1)(\Omega+2)$ characterizing the symmetric representation. This discrepancy can be solved again like in the simpler case of the nonrotating system by searching for the additional symmetry in the GCM energy matrix. Indeed, such a symmetry exists and is expressed by

$$H(\varphi',\psi';\varphi,\psi)=H(-\psi',-\varphi';-\psi,-\varphi) . \quad (51)$$

Owing to this symmetry one can split the representation space into two parts, a symmetric one

$$\Psi^{(s)}_{k,l}=\frac{1}{\sqrt{2(1+\delta_{k,-l})}} \times[\Phi_{k,l}(\varphi,\psi)+\Phi_{-l,-k}(\varphi,\psi)] , \quad (52)$$

and the antisymmetric part spanned by the eigenfunctions

$$\Psi^{(a)}_{k,l}=\frac{1}{\sqrt{2}}[\Phi_{k,l}(\varphi,\psi)-\Phi_{-l,-k}(\varphi,\psi)] . \quad (53)$$

Again, as in the previous case of the nonrotating system the symmetric subspace has the correct physical meaning and its dimension $\frac{1}{2}(\Omega+1)(\Omega+2)$ turns out to overlap precisely with that of the exact solution. The antisymmetric part can be neglected because $\Psi^{(a)}_{k,l}$ does not have a component with the correct number of particles.

D. Particle-number symmetry conserving GCM

It is well known[12] that the fluctuations coming from the Goldstone modes (connected with the particle-number nonconservation) can be taken into account exactly after performing the particle-number projection (PNP) before variation. The fact that the PNP method takes care of the bulk part of dynamic pairing correlations arises from the similarity between the RPA-like and the PNP-like wave functions (see, e.g. Ref. 10). In the case of the SO(5) model the PNP procedure can be performed analytically[26] and the corresponding result has turned out to be very close to the exact solution of the model.[6,26] In the GCM the superiority of the PNP generating functions over the standard HFB-like Slater determinants has been noticed long ago.[13–16] However, only very recently the particle-number conserving GCM has been employed to the case of nuclear rotation.[33] In the calculations of Ref. 33 the order parameter Δ has been used as a collective coordinate together with the projected HFBC generating functions. Unfortunately, because of the rather complex form of generating functions the solution of the GHW equations cannot be carried out analytically and the discretization method has to be used. The simple SO(5) model can be, therefore, a very good tool to investigate the usefulness of the discretization method as the kernels of the norm matrix and the Hamiltonian can be calculated analytically, as shown below.

The particle-number projection of the HFBC-type function can be performed by a simple multiplication of the Bogolyubov coefficients B by a factor $\exp(-2i\xi)$ and the integration over the gauge angle ξ,[12]

$$P^N|\Phi(A,B)\rangle=\frac{1}{2\pi}\int_0^{2\pi}d\xi\exp(iN\xi)|\Phi(A,\exp(-2i\xi)B)\rangle . \quad (54)$$

Therefore, to calculate the overlap matrix,

$$N(A',B';A,B)=\langle\Phi(A',B')|P^N|\Phi(A,B)\rangle =\frac{1}{2\pi}\int_0^{2\pi}d\xi\exp(iN\xi)\langle\Phi(A',B')|\Phi(A,\exp(-2i\xi)B)\rangle , \quad (55)$$

and the Hamiltonian kernels,

$$H(A',B';A,B)=\langle\Phi(A',B')|P^NHP^N|\Phi(A,B)\rangle =\frac{1}{2\pi}\int_0^{2\pi}d\xi\exp(iN\xi)\langle\Phi(A',B')|H|\Phi(A,\exp(-2i\xi)B)\rangle , \quad (56)$$

one can use the same formalism as given in Sec. III C. Moreover, the same symmetry properties for the Hamiltonian kernel hold here. After some lengthy calculations the kernels $N(\varphi',\psi';\varphi,\psi)$ and $H(\varphi',\psi';\varphi,\psi)$ can be found. The overlap kernel is given by

$$N(\varphi',\psi';\varphi,\psi)=F^{\Omega}_0(\alpha,\beta)=(\sqrt{\alpha\beta})^{\Omega}P_{\Omega}(z) , \quad (57)$$

where P_{Ω} is the Legendre polynomial of the order of Ω and

$$\alpha=\cos\frac{\varphi-\varphi'}{2}\cos\frac{\psi-\psi'}{2},\quad \beta=\cos\frac{\psi+\varphi'}{2}\cos\frac{\psi'+\varphi}{2},\quad z=\frac{|\alpha-\beta|}{2\sqrt{\alpha\beta}} , \quad (58)$$

$$F^p_d(x,y)=\frac{1}{2^{2p+1}}\sum_{k=0}^{p}\sum_{m=0}^{k}\binom{p}{k}\binom{2k}{m}\left[\binom{2(p-k)}{p-m+d}+\binom{2(p-k)}{p-m-d}\right](-1)^{m-k+d}x^k y^{p-k} . \quad (59)$$

The Hamiltonian kernel reads

$$\frac{H(\varphi',\psi';\varphi,\psi)}{N(\varphi',\psi';\varphi,\psi)} = -\epsilon\Omega F_0^{\Omega-1}(\alpha,\beta)a_1 - \omega\Omega F_0^{\Omega-1}(\alpha,\beta)a_2$$
$$-\tfrac{1}{8}G\Omega^2[F_0^{\Omega-2}(\alpha,\beta)(a_3+a_4)+F_1^{\Omega-2}(\alpha,\beta)(a_3-a_4)]$$
$$-\tfrac{1}{16}G\Omega[F_0^{\Omega-2}(\alpha,\beta)(a_5+a_6+2a_7)$$
$$+F_2^{\Omega-2}(\alpha,\beta)(a_5+a_6-2a_7)+2F_1^{\Omega-2}(\alpha,\beta)(a_5-a_6)]$$
$$-\tfrac{1}{2}\chi q^2\Omega^2 F_0^{\Omega-2}(\alpha,\beta)a_1^2 - \tfrac{1}{16}\chi q^2\Omega[F_0^{\Omega-2}(\alpha,\beta)(a_8+a_9+2a_1^2)$$
$$+F_2^{\Omega-2}(\alpha,\beta)(a_8+a_9-2a_1^2)+2F_1^{\Omega-2}(\alpha,\beta)(a_8-a_9)]$$
$$-\tfrac{1}{16}\chi q^2\Omega[F_0^{\Omega-2}(\alpha,\beta)(a_{10}-a_{11})+F_1^{\Omega-2}(\alpha,\beta)(a_{10}+a_{11})] , \tag{60}$$

where

$$a_1 = a_1(\varphi,\varphi';\psi,\psi') = \cos\frac{\psi+\varphi}{2}\cos\frac{\psi'-\varphi'}{2} + \cos\frac{\psi-\varphi}{2}\cos\frac{\psi'+\varphi'}{2} , \tag{61}$$

$$a_2 = a_2(\varphi,\varphi';\psi,\psi') = \cos\frac{\psi'-\varphi'}{2}\sin\frac{\varphi+\psi}{2} + \cos\frac{\psi-\varphi}{2}\sin\frac{\varphi'+\psi'}{2} , \tag{62}$$

$$a_3 = a_2^2(\varphi,\psi;\varphi',\psi'), \quad a_4 = a_2^2(\varphi,\varphi';-\psi,-\psi') , \tag{63}$$

$$a_5 = a_5(\varphi,\varphi';\psi,\psi') = \left[\cos\frac{\psi-\psi'}{2}\right]^2\cos\varphi\cos\varphi' + \left[\cos\frac{\varphi-\varphi'}{2}\right]^2\cos\psi\cos\psi'$$
$$+2\cos\frac{\psi-\psi'}{2}\cos\frac{\varphi-\varphi'}{2}\cos\frac{\varphi'-\psi'}{2}\cos\frac{\varphi-\psi}{2}, \quad a_6 = a_5(\varphi,-\psi';\psi,-\varphi') , \tag{64}$$

$$a_7 = a_5 - 2\cos\frac{\varphi-\varphi'}{2}\cos\frac{\psi-\psi'}{2}\sin\frac{\varphi'-\psi'}{2}\sin\frac{\varphi-\psi}{2} , \tag{65}$$

$$a_8 = a_8(\varphi,\varphi';\psi,\psi') = a_1^2 - 2\cos\frac{\varphi-\varphi'}{2}\cos\frac{\psi-\psi'}{2}\sin\frac{\varphi'+\psi'}{2}\sin\frac{\varphi+\psi}{2}, \quad a_9 = a_8(-\psi,-\varphi;\varphi',\psi') , \tag{66}$$

$$a_{10} = a_{10}(\varphi,\psi;\varphi',\psi') = -a_1^2 + a_5\left[\frac{\pi}{2}-\varphi',\frac{\pi}{2}-\psi;\frac{\pi}{2}-\varphi,\frac{\pi}{2}+\psi'\right]$$
$$+2\cos\frac{\varphi-\varphi'}{2}\cos\frac{\psi-\psi'}{2}\left[\cos\frac{\varphi-\psi'}{2}\cos\frac{\varphi'-\psi}{2} - \sin\frac{\varphi-\psi}{2}\sin\frac{\varphi'-\psi'}{2}\right] , \tag{67}$$

$$a_{11} = -a_{10}(-\psi,-\varphi;\varphi',\psi') . \tag{68}$$

In the RBCS limit (40) the above formulas are consistent with the PNP expressions of Ref. 26. The Griffin-Hill-Wheeler equation (2) is then solved by discretization.

IV. SOME EXAMPLES OF NUMERICALS RESULTS

In this section the main features of the GCM solutions of different versions of the two-level model are discussed. The first example illustrates the variant described in Sec. III B, i.e., $\hbar\omega=0$ case. The ground state energy in the case of $\Omega=2$, $\chi=0$, is plotted in Fig. 1 as a function of the pairing strength, G. The BCS solution and the result of the RPA calculations[6] are also shown for comparison. It is seen that the unprojected GCM energy behaves smoothly around the critical region of $G_{\rm crit}$ defined as

$$G_{\rm crit} = \frac{\epsilon}{\Omega} , \tag{69}$$

whereas the RPA curve shows a singularity at this point. At large values of pairing strength, however, the RPA

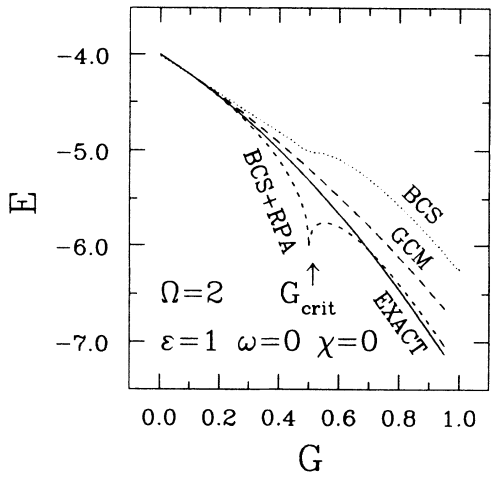

FIG. 1. The ground state energy of the two-level model as a function of G. The remaining parameters are $\Omega=2$, $\epsilon=1$, $\omega=0$, $\chi=0$. The solid line indicates the exact solution while the GCM result (Sec. III) is indicated by a long-dashed line. The BCS energy and the BCS+RPA solutions are indicated by dotted and short-dashed curves, respectively.

solution lies closer to the exact one than the GCM solution. This result is by no means surprising. In the RPA method the spurious made associated with the particle-number violation has been removed[6] while in the GCM case it gives an additional contribution to the energy which increases with G (see, e.g., Ref. 15).

In order to illustrate the structure of the GCM function let us consider the generating function for $\Omega=2$:

$$|\Phi,\Omega=2\rangle=\left[\sin^2\frac{\varphi}{2}+\cos^2\frac{\varphi}{2}P^{\dagger 2}_{\rm low}+\frac{1}{\sqrt{2}}\sin\varphi P^{\dagger}_{\rm low}\right]\times\left[\cos^2\frac{\varphi}{2}+\sin^2\frac{\varphi}{2}P^{\dagger 2}_{\rm up}+\frac{1}{\sqrt{2}}\sin\varphi P^{\dagger}_{\rm up}\right]|0\rangle\ , \tag{70}$$

where

$$P^{\dagger}_{\rm low}=\frac{1}{\sqrt{2}}\sum_{i=1}^{2}c^{\dagger}_{3i}c^{\dagger}_{4i},\quad P^{\dagger}_{\rm up}=\frac{1}{\sqrt{2}}\sum_{i=1}^{2}c^{\dagger}_{1i}c^{\dagger}_{2i} \tag{71}$$

are the pair creator operators for the lower and the upper level, respectively. The component with the good particle number ($N=4$) reads

$$|\Phi,\Omega=2,N=4\rangle=\left[\sin^4\frac{\varphi}{2}P^{\dagger 2}_{\rm up}+\cos^4\frac{\varphi}{2}P^{\dagger 2}_{\rm low}+\frac{1}{2}\sin^2\varphi P^{\dagger}_{\rm low}P^{\dagger}_{\rm up}\right]|0\rangle\ , \tag{72}$$

while the remaining part of the wave function (70) with $N=0,2,6,8$ particles is proportional to $\sin(\varphi)$.

In the limit of small G the weight function $f(\varphi)$ is peaked around $\varphi=0$, see Fig. 2, which corresponds to the almost full occupation of the lower level and the spurious component practically disappears. However, if $G\gg G_{\rm crit}$ the BCS theory gives a very similar occupation of both levels, thus $\varphi=\pi/2$. In this limit the spurious component enters the wave function with a maximal weight and, consequently, the difference between the GCM solution and the exact solution increases. The $G=2$ curve of Fig. 2 represents the case of a strong pairing. The maximum of the weight is very close to the BCS limit of $\varphi=0.42\pi$ given by Eq. (15). The transition point between these two regimes of pairing takes place at $G\approx 1.1$, see Fig. 2, which is much larger than $G_{\rm crit}=0.5$.

In the second example shown in Fig. 3 the influence of rotation is illustrated using the GCM variant discussed in Sec. III C. Here $\Omega=2$, $G=0.65$, and $\chi=0$. Like in the previous case the RPA solution collapses around the critical frequency of the two-level model given by

$$\omega_{\rm crit}=\epsilon\left[\left[\frac{G}{G_{\rm crit}}\right]^{2/3}-1\right]^{1/2}, \tag{73}$$

while the GCM gives a fairly good approximation to the exact energy. It is worth noting that even the anharmonic corrections to the RPA solutions obtained by means of the nuclear field theory[6] (denoted as NFT in Fig. 3) do not yield a better result as compared to GCM.

The two-parameter weight function is shown in Fig. 4 for $\Omega=2$, $\chi=0$, and $G=2$ (strong pairing at $\omega=0$). The diagram is symmetric with respect to the $\varphi=-\psi$ line as a result of the Hamiltonian symmetry (51). At $\omega=0$ the two symmetric maxima lie on the diagonal $\varphi=\psi$. They can be associated with the static pairing gap $\Delta_{\rm static}\neq 0$.

At high frequency $\hbar\omega=2.4$ only one maximum is seen on the $\varphi=-\psi$ line which can be associated with $\Delta_{\rm static}=0$. In this case the reflection symmetry with respect to the diagonal $\varphi=\psi$, related to the time reversal invariance, is broken. The corresponding RBCS values of generator coordinates [Eq. (41)] are indicated by the

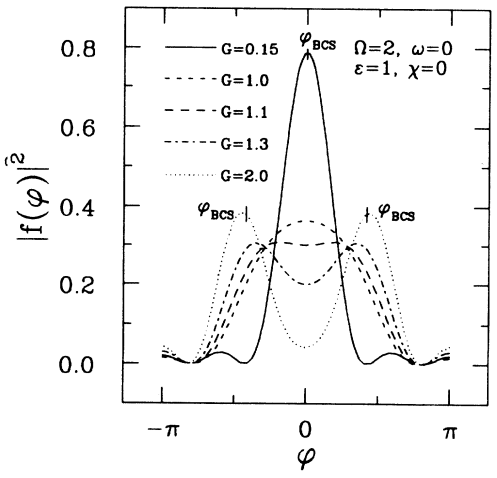

FIG. 2. The weight functions $f(\varphi)$ of the GCM ground state of the simple model for different values of G. The corresponding BCS values of φ ($\varphi_{\rm BCS}$) given by Eq. (15) are also given in the cases of small ($\varphi_{\rm BCS}\approx 0$) and large ($\varphi_{\rm BCS}\approx 0.42\pi$) pairing.

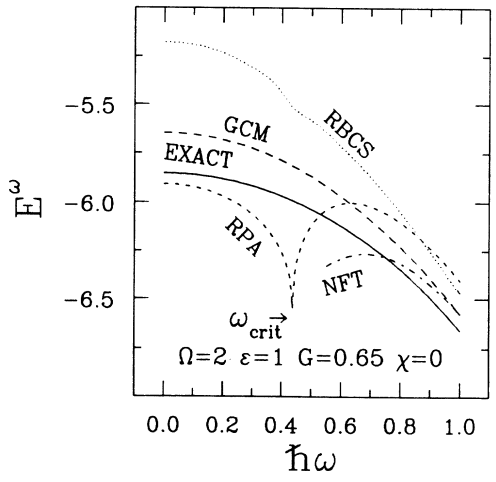

FIG. 3. The lowest Routhians for the GCM, RPA, RBCS, and exact solutions of the model versus rotational frequency ω. The parameters are $\Omega=2$, $G=0.65$, $\epsilon=1$, $\chi=0$. The curve indicated as NFT contains anharmonic corrections to the ground state RPA energy.

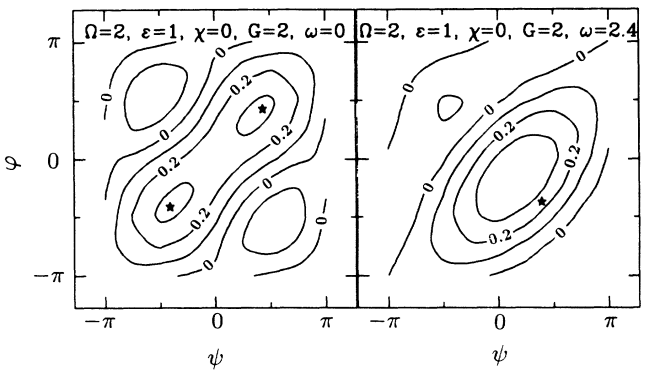

FIG. 4. The weight function $f(\varphi,\psi)$ of the GCM ground state of the two-level model. The left diagram corresponds to $\omega=0$ while the case of a very fast rotation is presented in the right portion. The stars indicate the corresponding RBCS values of generator coordinates given by Eq. (41).

stars. They are quite close to the maxima of the weight function.

The last example deals with the full version of the model (Sec. III C). A special emphasis is put on the two lowest excited states calculated relatively to the ground state in the rotating frame. The energy values obtained within the GCM are compared to the exact solutions of the model and to the results of the RPA.[34] Figure 5 gives the variation of the energies as a function of rotational frequency ω for the following parameter set:

$$\epsilon=1,\quad G=0.2,\quad \chi=0.02,\quad q=1,\quad \Omega=10\ . \tag{74}$$

The variation of the pairing gap Δ vs ω is also shown in the inset of Fig. 5. The present case corresponds to a situation of a "strong pairing":[25] the curve $\Delta=\Delta(\omega)$ exhibits a two-valued dependence in the narrow region of ω ($\omega_c<\omega<\omega_r$). The existence of such a region is related to the peculiar choice of the parameter set (74). As seen from the figure, the exact solution for the first excited state presents the minimum in the neighborhood of ω_c. The RPA approach overestimates the energy of the lowest excitation for low values of ω. Furthermore, the RPA energy, ω_M, goes to zero for a value ω_Ω slightly greater than ω_c. We may add here that there exist also two gapless RPA solutions. A first one, 2Λ, corresponds to the tow phonon state containing one addition and one removal phonon. It starts at ω_c and rises very quickly with ω finally approaching the second excited state of the exact version of the model. The second one, S exists for all values of the rotational frequency. It gets a physical meaning only for $\omega>\omega_c$ and it corresponds to the quadrupole β vibrations depending essentially on the strength χ of the Q-Q force. Consequently, the RPA approach does not provide us with a continuous description of the physical situation through the region where the pairing collapses. On the other hand, the GCM solution (dashed line) appears as much better approximation. The variation of the GCM solution follows that of the exact version and for the small and large values of ω the GCM solution is also very close to the exact curve. The same is also true for the next excited state. Through the whole region the GCM improves the description as compared to RPA. This appears to be a general property as we shall see in the forthcoming paper.[35] If the particle-number projection procedure is employed the GCM solution discussed in Sec. III D overlaps with the exact solutions of the model not only for the ground state configuration but also for the all excited states.

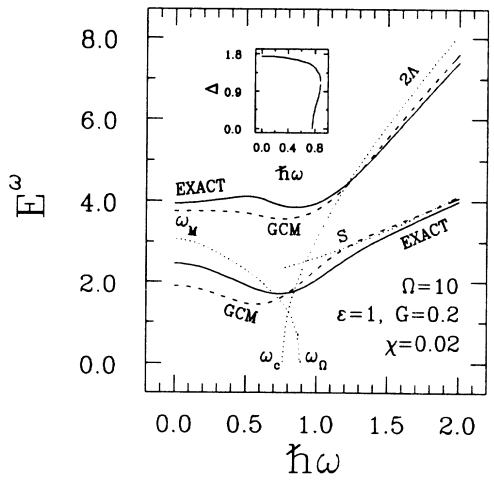

FIG. 5. The first and the second excited state of the two-level model as a function of $\hbar\omega$. The parameters are $\Omega=10$, $G=0.2$, $\epsilon=1$, $q=1$, $\chi=0.02$. The RPA solutions (dotted lines) and the GCM solution (dashed line) are compared to the exact result (solid line). The corresponding RBCS pairing gap is shown in the inset as a function of $\hbar\omega$. For more details see text.

V. SUMMARY AND CONCLUSIONS

We employed the GCM to the rotating two-level model to discuss the behavior of pair correlations at high spins. The main conclusions can be summarized as follows:

(i) The GCM reproduces fairly well the excitation spectrum of the two-level model. Unlike the RPA approach which breaks down in the region of the pairing collapse the GCM offers a smooth transition between the region of a static pairing (pairing rotation) and the vibrational region where the dynamical fluctuations dominate.

(ii) The RBCS-like generating wave function parametrized by means of the two generator coordinates gives a satisfactory description of the lowest $K=0$ collective excitations of the model which can be related to the pairing and quadrupole vibrations.

(iii) The dimension of the Hilbert space associated with the symmetric representation of the exact solution of the simple model is exactly the same as the dimension of the symmetric collective subspace of GCM. The collective GCM subspace spanned on the asymmetric wave functions seems to be unphysical as it does not contain the component with the proper number of particles.

(iv) The energy spectrum of the SO(5) model obtained

with the particle-number symmetry conserving GCM overlaps with that of the exact solution, if the sufficient number of the grid points in the discretization method is used. The detailed discussion of the convergence problem will be given in a forthcoming article.[35]

ACKNOWLEDGMENTS

This work was supported in part by the Polish Ministry of National Education under Contract CPBP 01.09. One of us (W.S.) is grateful to the Swedish Natural Research Council and Göran Gustafsson Foundation for the financial support during his stay at Manne Siegbahn Institute of Physics in Stockholm where part of this work was performed. The other (Z.S.) wishes to acknowledge a visit in the Institut des Sciences Nucléaires in Grenoble and the very good working conditions there. This work was carried out under the Institut Nacional de Physique Nucléaire et de Physique des Particules–Warsaw University cooperation agreement.

[1]A. Bohr and B. R. Mottelson, *Nuclear Structure* (Benjamin, New York, 1975), Vol II.
[2]A. Bohr and B. R. Mottelson, Phys. Scr. **24**, 71 (1981).
[3]B. R. Mottleson and J. G. Valatin, Phys. Rev. Lett. **5**, 511 (1960).
[4]R. A. Broglia, M. Diebel, S. Frauendorf, and M. Gallardo, Phys. Lett. **166B**, 252 (1986).
[5]Y. R. Shimizu, R. Vigezzi, and R. A. Broglia, Phys. Lett. B **198**, 33 (1987).
[6]D. Bes, R. A. Broglia, J. Dudek, W. Nazarewicz, and Z. Szymański, Ann. Phys. (N.Y.) **182**, 237 (1988).
[7]S. Bose, J. Krumlinde, and E. R. Marshalek, Phys. Lett. **53B**, 136 (1974).
[8]S. Y. Chu, E. R. Marshalek, P. Ring, J. Krumlinde, and J. O. Rasmussen, Phys. Rev. C **12**, 1017 (1975).
[9]Y. R. Shimizu and R. A. Broglia, Nucl. Phys. **A476**, 228 (1988).
[10]Y. R. Shimizu, J. D. Garrett, R. A. Broglia, M. Gallardo, and E. Vigezzi, Rev. Mod. Phys. **61**, 131 (1989).
[11]P. Ring, in *Contemporary Topics in Nuclear Structure Physics,* edited by R. F. Casten, A. Frank, M. Moshinsky, and S. Pittel (World Scientific, Singapore, 1988), p. 677.
[12]P. Ring and P. Schuck, *The Nuclear Many-Body Problem* (Springer-Verlag, New York, 1980), Chap. 10 and Appendix E.
[13]D. Justin, M. V. Mihailović, and M. Rosina, Phys. Lett. **29B**, 458 (1969).
[14]C. D. Siegal and R. A. Sorensen, Nucl. Phys. **A184**, 81 (1972).
[15]R. A. Sorensen, Phys. Lett. **38B**, 376 (1972).
[16]A. Faessler, F. Grümmer, and A. Plastino, Z. Phys. **260**, 305 (1973).
[17]M. Didong, H. Müther, K. Goeke, and A. Faessler, Phys. Rev. C **14**, 1189 (1976).
[18]T. Une, A. Ikeda, and N. Onishi, Prog. Theor. Phys. **55**, 498 (1976).
[19]F. Villars, Nucl. Phys. **A285**, 269 (1977).
[20]M. Baranger and M. Véneroni, Ann. Phys. (N.Y.) **114**, 123 (1978).
[21]O. Civitarese, A. Plastino, and A. Faessler, Z. Phys. A **313**, 197 (1983).
[22]A. Góźdź and K. Pomorski, Nucl. Phys. **A451**, 1 (1986).
[23]M. Kyotoku and H. T. Chen, Phys. Rev. C **36**, 1144 (1987).
[24]J. Krumlinde and Z. Szymański, Ann. Phys. (N.Y.) **79**, 201 (1973).
[25]Z. Szymański, in *Nuclear Physics with Heavy Ions and Mesons,* Les Houches, Session XXX, 1977, edited by R. Balian, M. Rho, and G. Ripka (North-Holland, Amsterdam, 1977), p. 297.
[26]W. Nazarewicz, J. Dudek, and Z. Szymański, Nucl. Phys. **A436**, 139 (1985).
[27]D. L. Hill and J. A. Wheeler, Phys. Rev. **89**, 1102 (1953).
[28]J. J. Griffin and J. A. Wheeler, Phys. Rev. **108**, 311 (1957).
[29]F. Dönau, J.-Y. Zhang, and L. L. Riedinger, Nucl. Phys. **A496**, 333 (1989).
[30]J. Krumlinde and Z. Szymański, Phys. Lett. **36B**, 157 (1971).
[31]R. Piepenbring, B. Silvestre-Brac, and Z. Szymański, Nucl. Phys. **A349**, 77 (1980).
[32]N. Onishi and S. Yoshida, Nucl. Phys. **80**, 367 (1966).
[33]L. F. Canto, P. Ring, and J. O. Rasmussen, Phys. Lett. **161B**, 21 (1985).
[34]R. Piepenbring and Z. Szymański, Nucl. Phys. A (to be published).
[35]W. Satuła, W. Nazarewicz, R. Piepenbring, and Z. Szymański (unpublished).